EFFECTS OF SOIL SPATIAL VARIABILITY ON LIQUEFACTION BEHAVIOR OF HORIZONTALLY LAYERED GROUND

Vargas Tapia Ruben Rodrigo[1], Kyohei UEDA[2] and Susumu IAI[3]

[1]Research student, Disaster Prevention Research Institutte, Kyoto University
(Gokasho, Uji, Kyoto 611-0011, Japan)
E-mail: vargas.rodrigo.35m@st.kyoto-u.ac.jp
[2]Member of JSCE, Assistant Professor, Disaster Prevention Research Institutte, Kyoto University
(Gokasho, Uji, Kyoto 611-0011, Japan)
E-mail: ueda.kyohei.2v@kyoto-u.ac.jp
[3]Member of JSCE, Professor, Disaster Prevention Research Institute, Kyoto University
(Gokasho, Uji, Kyoto 611-0011, Japan)
E-mail: iai.susumu.6x@kyoto-u.ac.jp

Effective stress analyses based on the finite element method are often used as a reliable tool to predict liquefaction occurrence in soil-structure systems during earthquakes. In the analyses, the soil properties are typically specified by using a deterministic model although they intrinsically have spatial variability even in the case of horizontally layered ground. In this study, nonlinear finite element analyses are performed to investigate the effects of soil heterogeneity on the liquefaction behavior of stochastically heterogeneous soil deposits subjected to seismic loading through a Monte Carlo simulation approach. A series of analyses has revealed that the heterogeneity of the shear wave velocity (or initial shear modulus) has no significant effect on the distribution of the computed excess pore water pressure (EPWP), while the maximum value of EPWP ratio is partially influenced and becomes less by considering the spatial variability in the internal friction angle and the *N* value under the given seismic loading.

Key Words : *liquefaction, spatial variability, effective stress analysis*

1. INTRODUCTION

In order to predict the liquefaction potential and liquefaction-induced damage to soil-structure systems during earthquakes, effective stress analyses based on the finite element method are often used as a reliable tool in seismic design. The analyses require accurate modeling of liquefiable ground properties (e.g. cyclic shear strength), which greatly affect the numerical results. Although the soil properties are typically specified by using deterministic (uniform) models in the standard design, they intrinsically have spatial variability even in the case of horizontally layered ground. In addition, the heterogeneity of soil properties has been proven to affect the dynamic behavior of ground and to induce significant variability in the predicted response for some cases (Popescu et al. 1997; 2005, Montgomery and Boulanger 2016). However, the effect has not yet been fully studied in a quantitative way.

In this study, two-dimensional nonlinear finite element analyses are carried out to investigate the effects of soil heterogeneity on the liquefaction potential and dynamic response of stochastically heterogeneous soil deposits subjected to seismic loading. The analyses build on a Monte Carlo simulation approach following Popescu et al. (1997). The material nonlinearity of soils is expressed by using a strain space multiple mechanism model (Iai et al. 1992) proposed by one of the authors. Numerical simulation procedures using the model in the finite element program FLIP (Iai et al. 1992; 1998) are described. In the simulation, the spatial distribution of the SPT N_1 value, the shear wave velocity (i.e. shear modulus) and the internal friction angles in the liquefiable deposits are separately taken into account by using sample functions of discretized triangular and exponential stochastic fields (Kanda and Motosaka 1995) in addition to Gaussian one. Simulation results for stochastic models are compared to those for deterministic models by focusing on ground lateral displacement and excess pore water pressure

(EPWP) build-up.

2. MODELING OF SPATIAL VARIABILITY OF SOIL PROPERTIES

The SPT N1 value, shear wave velocity (V_s), and internal friction angle (ϕ_f) are separately considered as probabilistic variables in this study. That is to say, only one property among them expresses the variability with the other two properties kept constant for simplicity, although correlation between shear wave velocity and friction angle has been pointed out (e.g. Andrus and Stokoe 2000). However, when the SPT N1 value is considered to be a stochastic field, the other two properties automatically vary following a simplified method for parameter identification of FLIP program (Morita et al. 1997, Mikami et al. 2011) as described later.

For the each soil property, a one-variate, two-dimensional (1V-2D) stochastic field (Vanmarcke 1984), which produces the probability and cumulative distribution functions (PDF, CDF), is required in order to perform stochastic analyses. In this study, nine sample functions of the 1V-2D field are generated for the Monte Carlo simulation by using sample functions of discretized Gaussian, triangular, and exponential stochastic fields. In other words, each type of stochastic fields creates three possible realizations for the each soil property over the analysis domain.

Spectral density functions of the two-dimensional stochastic fields are given as shown in Table 1 by applying the following Wiener-Khinchin theorem (Kanda and Motosaka 1995)

$$S = \frac{1}{(2\pi)^2} \int_{-\infty}^{\infty}\int_{-\infty}^{\infty} R \exp\left\{-i\left(\kappa_x \xi_x + \kappa_y \xi_y\right)\right\} d\xi_x d\xi_y \quad (1)$$

where $R(\xi_x, \xi_y)$ is the correlation function (CF) of the stochastic fields, ξ_x ($=x_1$-x_2) and ξ_y ($=y_1$-y_2) is the distance between two points in x and y direction, respectively, and $\boldsymbol{\kappa}=(\kappa_x, \kappa_y)^T$ is a wave number vector. In Table1, σ denotes the standard deviation of variational parameters, and dx, dy is the correlation distance in x and y direction, respectively. By following Nadim et al. (2005), dx=10.0 m and dy=1.0 m were used in this study.

According to Shinozuka and Deodatis (1996), a random process following the spectral density functions are derived, by assuming the mean value is zero, as follows:

$$f(x,y) = \sqrt{2}\sum_{k=1}^{K_x}\sum_{l=1}^{K_y} A_{kl} \times\left[\cos\left(\kappa_{xk}x + \kappa_{yl}y + \Phi_{kl}^{(1)}\right) + \cos\left(\kappa_{xk}x - \kappa_{yl}y + \Phi_{kl}^{(2)}\right)\right] \quad (2)$$

$$A_{kl} = \sqrt{2S\left(\kappa_{xk}, \kappa_{yl}\right)\Delta\kappa_x\Delta\kappa_y} \quad (3)$$

where Φ_{kl} is an independent random phase angle distributed with uniformity between 0 and 2π. K_x and K_y is the division number for calculating wave number in x and y direction, respectively, and may be different from the division number of finite element mesh, and $\Delta\boldsymbol{\kappa}=(\Delta\kappa_x, \Delta\kappa_y)^T$ is an incremental vector of wave number. In this study, K_x=K_y=1000 and $\Delta\kappa_x$=$\Delta\kappa_y$=0.01 were used. Finally, the spatial distribution F of stochastic variables representing the heterogeneity of soil properties is given as follows:

Table 1 Spectral density functions of two-dimensional stochastic fields.

Type	Spectral density function $S\left(\kappa_x, \kappa_y\right)$
Gaussian	$\sigma^2 \cdot \frac{d_x d_y}{4\pi} \cdot \exp\left\{-\left(\frac{d_x^2}{4}\kappa_x^2 + \frac{d_y^2}{4}\kappa_y^2\right)\right\}$
Triangular	$\sigma^2 \cdot \frac{4\sin^2\left(d_x\kappa_x/2\right)\sin^2\left(d_y\kappa_y/2\right)}{\pi^2 d_x d_y \kappa_x^2 \kappa_y^2}$
Exponential	$\sigma^2 \cdot \frac{1}{(2\pi)^2} \cdot \left(\frac{2d_x}{d_x^2\kappa_x^2+1}\right)\left(\frac{2d_y}{d_y^2\kappa_y^2+1}\right)$

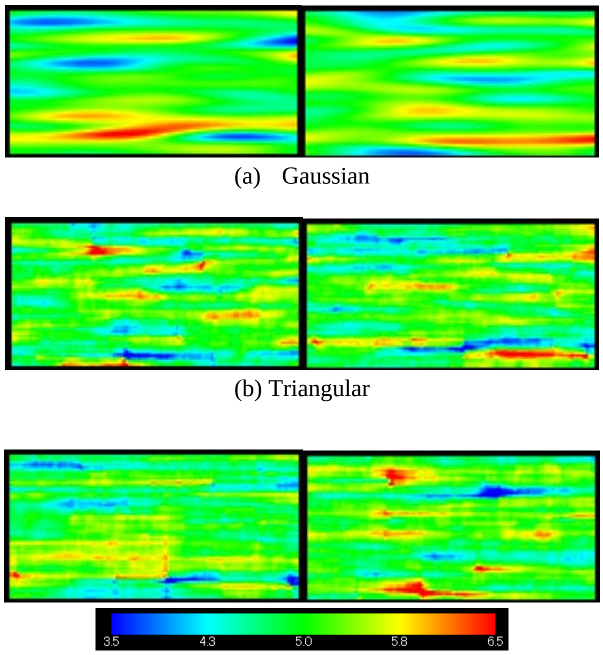

(a) Gaussian

(b) Triangular

(c) Exponential

Figure 1 Spatial distribution of SPT N_1 value.

3. NUMERICAL SIMULATION PROCEDURE

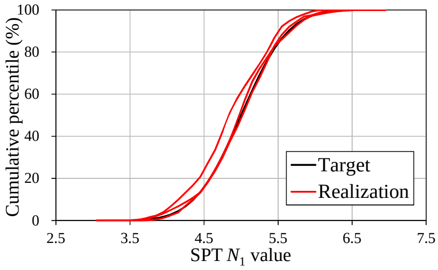

(a) Gaussian

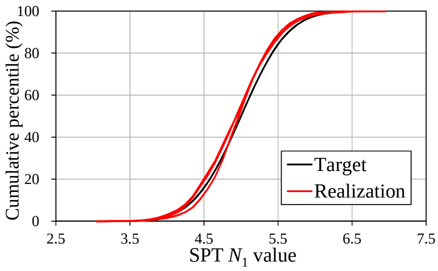

(b) Triangular

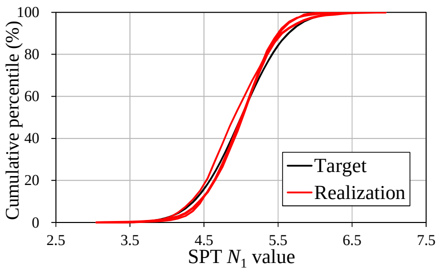

(c) Exponential

Figure 2 Cumulative distribution function for N_1.

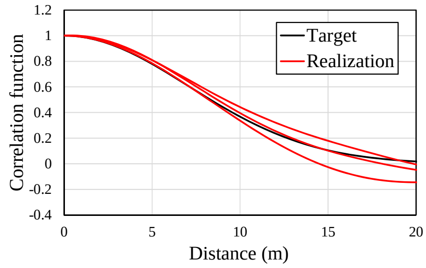

(a) Gaussian

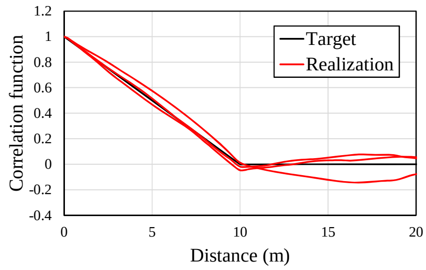

(b) Triangular

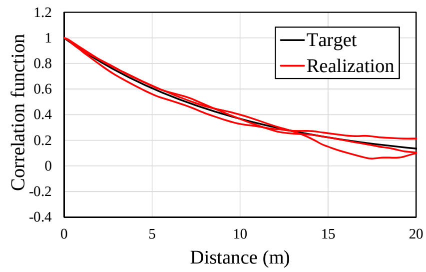

(c) Exponential

Figure 3 Correlation function for N_1.

Two dimensional nonlinear seismic response analyses were performed on a liquefiable sand deposit shown in Fig. 4 using a finite element program for soil-structure systems (FLIP) (Iai et al. 1992; 1998). The finite element mesh has 64 rows with 128 columns, for a total of 16,384 elements (including 8,192 pore water elements). The liquefiable deposit, consisting of clean sand, was modeled using a strain space multiple mechanism model, called multi-spring model (Iai et al. 1992). Model parameters (e.g. initial shear modulus ($G_{ma}=\rho V_s^2$), internal friction angle (ϕ_f)), including dilatancy parameters, were determined by a simplified method for parameter identification of FLIP program (Morita et al. 1997, Mikami et al. 2011) based on the SPT N value (=5 in this study) with effective overburden pressure (=98 kPa) and fines content (=0%). Simulated liquefaction resistance curve is shown in Fig. 5 with the cases of N=10 and 15.

The boundary conditions for displacement were selected to replicate horizontally layered ground. The displacement degrees of freedom on the left side boundary were slaved to move together with their counterparts on the right boundary. Rigid base boundaries were used at the bottom of the model, with the input motion shown in Fig. 6. The ground water table was set at the ground surface. In the simulation, stochastic variability for the SPT N_1 value, the shear wave velocity (V_s), and the internal friction angle (ϕ_f) described in the previous section was separately taken into account to investigate the effects of soil heterogeneity on the dynamic response of stochastically heterogeneous liquefiable deposits subjected to seismic loading. The simulation was carried out under undrained condition, and thus the ground settlement after shaking is out of scope in this study.

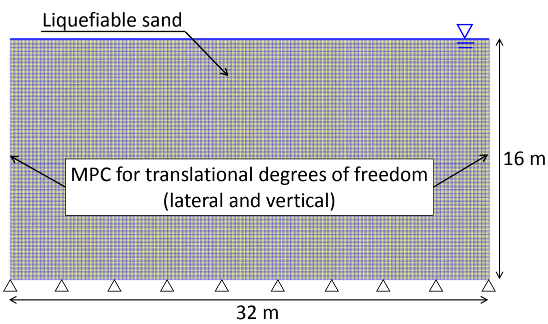

Figure 4 Finite element mesh of horizontally layered liquefiable ground.

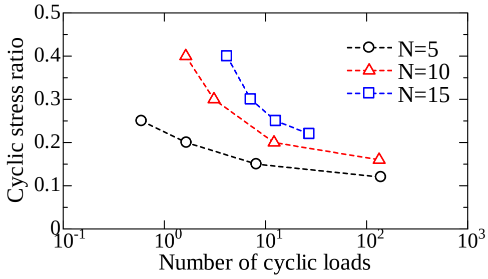

Figure 5 Liquefaction resistance curve.

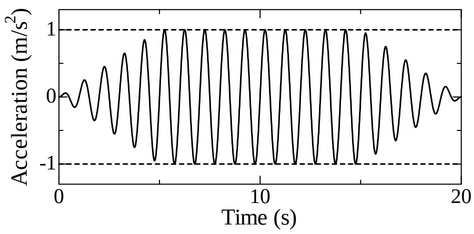

Figure 6 Input ground motion.

4. ANALYSIS RESULTS

(1) Maximum Lateral Displacement

The variations of maximum lateral displacement at the right (or left) boundary with depth are shown in Fig. 7 with the results of three uniform (i.e. deterministic) models. For each stochastic model, an averaged profile over three realizations is depicted. When the SPT N_1 value is treated as a stochastic variable (see Figs. 1 through 3), a similar profile is obtained regardless of the type of stochastic fields in Fig. 7(a). The surface displacements for these stochastic realizations are less than those for uniform models with N_1 value between the 20th and 80th percentiles. This may be because a domain-averaged EPWP ratio in the stochastic models is less than that in the deterministic models as shown in Fig. 9(a) later and the difference affects the shear strain development.

When the shear wave velocity and internal friction angle are treated as a stochastic variable, the difference in the type of stochastic fields has no significant effect on the displacement profiles (Fig. 7(b)(c)) as is the case with the SPT N_1 value. Figure 7(c) indicates that The surface displacements for the stochastic realizations are closest to that for a uniform model with an internal friction angle of the 20th percentile (ϕ_f=31.2 degree), but the precise representative ϕ_f value is currently hard to be specified because whether less percentile values give a closer profile to the stochastic cases was not tested. The less surface displacements in the stochastic models may be due to the difference in the averaged EPWP ratio between the deterministic and stochastic models as shown in Fig. 9(c). When the shear wave velocity is variable,

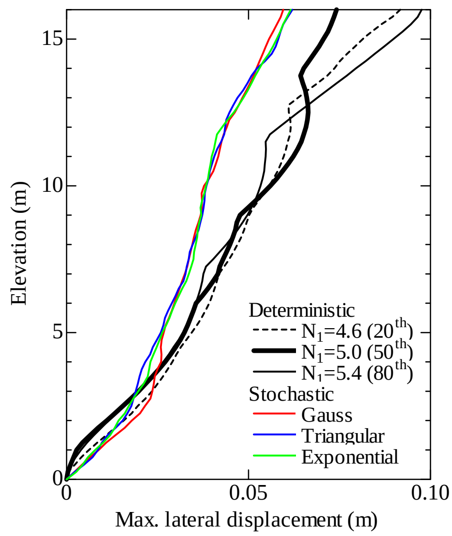

(a) The case of variable SPT N_1 value

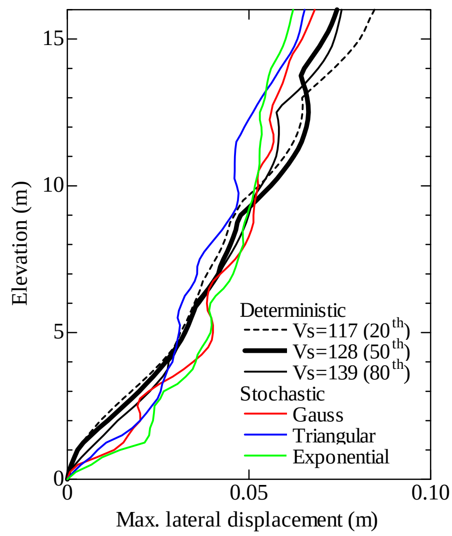

(b) The case of variable shear wave velocity

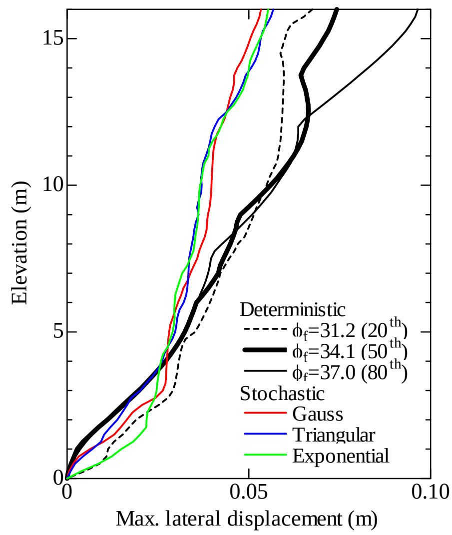

(c) The case of variable internal friction angle

Figure 7 Maximum lateral displacement profiles.

the 50th percentile is closest to the stochastic models in Fig. 7(b) focusing on the ground surface response. However, the discrepancy among the three uniform models is not so large. Thus, the heterogeneity of shear wave velocity (or initial shear modulus) is considered to have no significant effect on lateral displacement profiles.

(2) Excess Pore Water Pressure Ratio

Time history of simulated EPWP ratio is shown in Figs. 8 and 9. Figure 8 shows the largest value (P_{max}) among 8,192 soil elements while Fig. 9 does the domain-averaged value (P_{ave}) over the elements. The difference between P_{max} and P_{ave} is considered to indicate the magnitude in the simulated EPWP variation in location. When the SPT N_1 value is treated as a stochastic variable, a similar response is observed regardless of the type of stochastic fields in Figs. 8(a) and 9(a) as is the case with the lateral displacement profiles. P_{max} eventually results in the same value (=0.97) after shaking between the uniform and stochastic models, although the build-up process is different during shaking (Fig. 8(a)). In contrast, a final value of P_{ave} in the stochastic models is about 0.1 smaller than that in the uniform models between the 20th and 80th percentiles (Fig. 9(a)).

The comparison of the time history of EPWP ratio for stochastic and deterministic models in Figs. 8(a) and 9(a) with the lateral displacement profiles in Fig. 7 illustrate how the representative N_1 value depends on the specific response measure and the timing of concern. Different from the value for the lateral displacement profiles, the representative N_1 value is almost the same as the mean N_1 value (i.e. the 50th percentile) during and after shaking if P_{max} is the response measure of concern. In contrast, the representative N_1 value varies depending on the timing if P_{ave} is the response measure of concern. After 3 s, we cannot find the representative value between the 20th and 80th percentiles.

When the shear wave velocity is treated as a stochastic variable, no significant difference is recognized among the uniform and stochastic models for both P_{max} and P_{ave} shown in Figs. 8(b) and 9(b), respectively, as is the case with the lateral displacement profiles (Fig. 7(b)). This is because the variation of shear wave velocity (or Initial shear modulus) may only affect linear elastic behavior within a small strain range, whereas a strength parameter (e.g. internal friction angle, undrained shear strength at steady state) is thought to exercise a dominant influence on nonlinear behavior such as liquefaction.

Figures 8(c) and 9(c) show the time history of EPWP ratio obtained from stochastic simulations in which the variability of internal friction angle is taken into account. The overall trend is similar to the case of SPT N_1 value being a stochastic variable (Figs. 8(a) and 9(a)). As described in a former paragraph, the representative ϕ_f value depends on the specific response measure and the timing of concern. The ϕ_f value is between the 20th and 50th percentiles during shaking and almost the same as the mean N_1 value after shaking if P_{max} is the response measure of concern. In contrast, no difference is observed before 3 s among the three uniform and three stochastic models when P_{ave} is the response measure of concern. The difference of the uniform and stochastic models becomes larger and larger between 3 and 5 s, and is kept constant after 5 s up to the end of shaking. The final difference of P_{ave} is between 0.15 and 0.2, which are larger than that in the case of SPT N_1 value

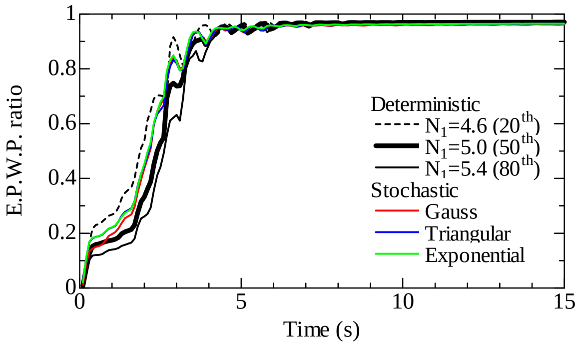

(a) The case of variable SPT N_1 value

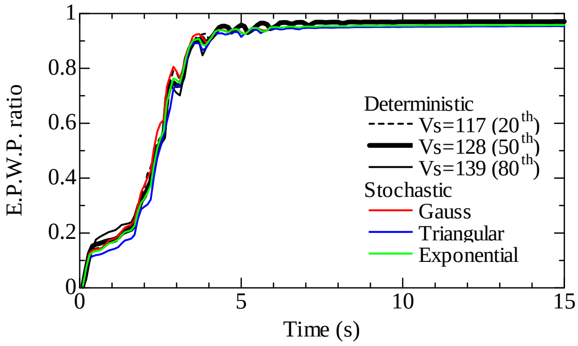

(b) The case of variable shear wave velocity

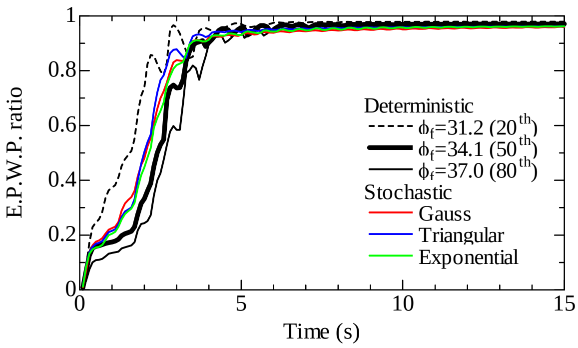

(c) The case of variable internal friction angle

Figure 8 Time history of maximum EPWP ratio.

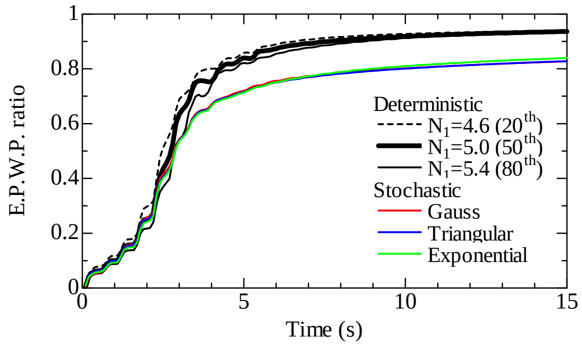

(a) The case of variable SPT N_1 value

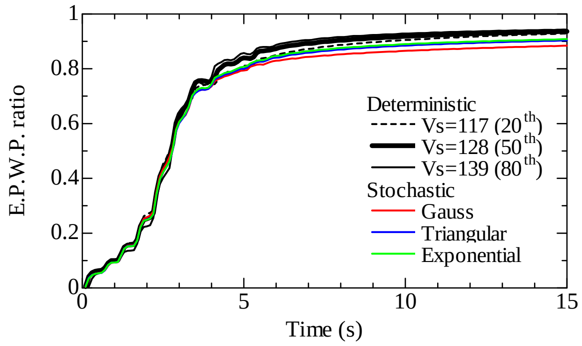

(b) The case of variable shear wave velocity

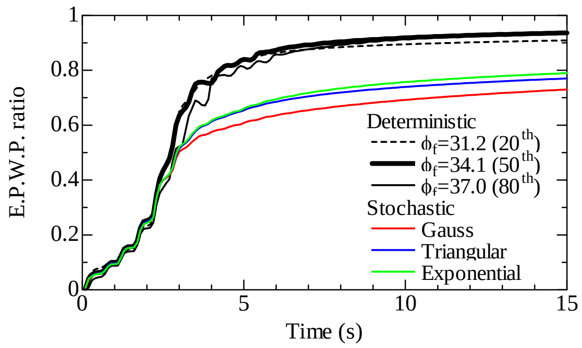

(c) The case of variable internal friction angle

Figure 9 Time history of averaged EPWP ratio.

being a stochastic variable (Fig. 9(a)).

Figure 10 shows some examples of the distribution of EPWP ratio after shaking when the SPT N_1 value is treated as a stochastic variable. Each figure corresponds to the counterpart in Fig. 1 (e.g. the left figure in Fig. 10(a) was obtained using the spatial distribution located on the left side of Fig. 1(a)). Whereas uniform distribution of EPWP ratio (=0.97) is obtained except for the bottom layer of the analytical domain in the deterministic model, the contrast between looser (i.e. higher EPWP ratio) and denser zones (i.e. lower EPWP ratio) is clearly recognized in the stochastic models. The difference among the three types of stochastic fields in Fig. 10 has a superficial similarity to that of the spatial distribution of SPT N_1 value shown in Fig. 1. Therefore, the distribution of EPWP ratio after shaking is considered to be affected by the spatial variability of input soil parameters. The reason EPWP is locally hard to build up in the case of stochastic models may be that liquefaction of locally looser zones (see Fig. 1) decreases the amount of shear stress (or acceleration) on surrounding denser zones essentially having higher resistance to liquefaction. This interpretation may hold only in the given condition (e.g. soil properties such as SPT N_1 value, model geometry, input motions), and further studies are required in order to clarify whether deterministic models are more prone to liquefaction than stochastic ones under other conditions.

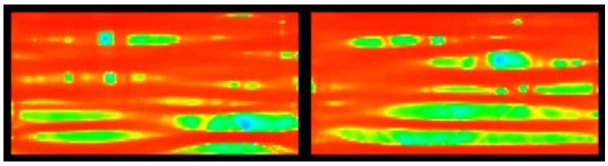

(a) Stochastic model: Gaussian

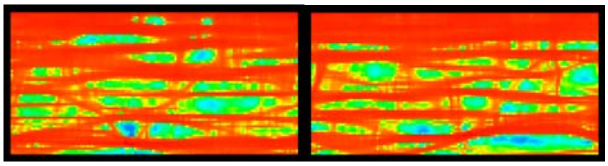

(b) Stochastic model: Triangular

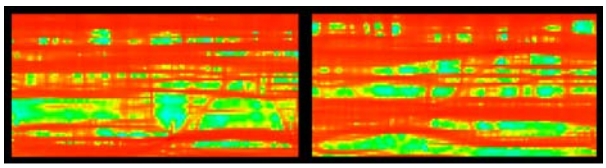

(c) Stochastic model: Exponential

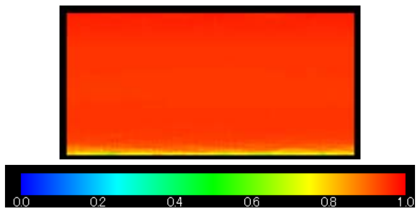

(d) Deterministic model (N_1=5)

Figure 10 Distribution of EPWP ratio after shaking (the case of variable SPT N_1 value).

5. CONCLUSIONS

The effects of soil heterogeneity on the liquefaction potential and dynamic response of stochastically heterogeneous soil deposits was examined using two-dimensional nonlinear seismic response analyses. In order to consider the spatial variability of soil properties, three types of sample functions (i.e. Gaussian, triangular, and exponential) of discretized stochastic fields were used for the spatial distribution of the SPT N_1 value, shear wave velocity, and internal friction angle in the liquefiable deposits.

A series of the analyses has revealed that the heterogeneity of shear modulus has no significant effect on the maximum lateral displacement profiles and the distribution of excess pore water pressure ratio if other parameters remain constant. In contrast, the results were influenced by the spatial variability in SPT N value and internal friction angle. The average value of excess pore water pressure ratio for the stochastic models became less than that for the deterministic models. In particular, the heterogeneity of internal friction angle has been recognized to reduce the average value to about 80 % of that in the case of homogeneity. This is because the variation of shear wave velocity (or Initial shear modulus) may only affect linear elastic behavior, whereas a strength parameter (e.g. internal friction angle) is considered to exercise a dominant influence on nonlinear behavior such as liquefaction.

Comparison between the stochastic and deterministic models has illustrated how the representative value depends on the specific response measure and the timing of concern. When the SPT N_1 value and the internal friction angle were treated as a stochastic variable for loose sandy ground, the lateral displacements for the stochastic realizations were out of the range between the 20th and 80th percentiles. With regard to the time history of excess pore water pressure ratio, the representative N_1 value was almost the same as a mean N_1 value (i.e. the 50th percentile) if the maximum value of excess pore water pressure ratio during and after shaking was the response measure of concern. In contrast, the representative value has been confirmed to vary depending on the timing if the average value of excess pore water pressure ratio is the response measure of concern.

The consequence obtained from this study may hold only in the given analytical conditions (e.g. soil properties such as SPT N_1 value, model geometry, input motions). Thus, further studies are required in order to clarify whether stochastic models are more prone to liquefaction than deterministic ones under other conditions.

REFERENCES

1) Andrus, R. D. and Stokoe II, K. H.: Liquefaction resistance of soils from shear-wave velocity, Journal of Geotechnical and Geoenvironmental Engineering, 126(11), 1015-1025, 2000.
2) Iai, S., Ichii, K., Liu, H. and Morita, T.: Effective Stress Analyses of Port Structures, Soils and Foundations, Special Issue on Geotechnical Aspects of the January 17 1995 Hyogoken-Nambu Earthquake, 2, 97-114, 1998.
3) Iai, S., Matsunaga, Y. and Kameoka, T.: Space Plasticity Model for Cyclic Mobility, Soils and Foundations, 32(2), 1-15, 1992.
4) Kanda, K. and Motosaka, M.: The Evaluation of Effects of Spatial Variability of Soil Properties, Surface Topography and Spatial Coherency of Incident Wave on Ground Motion Amplification –The Case of Kushiro J.M.A. Site–, J. Struct. Constr. Eng., AIJ, 476, 85-94, 1995 (in Japanese).
5) Mikami, T., Ozutsumi, O., Nakahara, T., Iai, S., Ichii, K. and Kawasaki, T.: Easy method for setting parameters of liquefaction analysis program FLIP, the 46th Japan National Conference on Geotechnical Engineering, Kobe, Japan, 1627-1628, 2011 (in Japanese).
6) Montgomery, J. and Boulanger, R. W.: Effects of Spatial Variability on Liquefaction-Induced Settlement and Lateral Spreading, Journal of Geotechnical and Geoenvironmental Engineering, 2016 (http://dx.doi.org/10.1061/(ASCE)GT.1943-5606.0001584 in press).
7) Morita, T., Iai, S., Liu, H., Ichii, K. and Sato, Y.: Simplified Method to Determine Parameter of FLIP, Technical Note of the Port and Airport Research Institute, No. 869, 1997 (in Japanese).
8) Nadim, F., Einstein, H. and RoBerds, W.: Probabilistic Stability Analysis for Individual Slope in Soil and Rock, Proc. Int. Conf. on Landslide Risk Management, 63-98, 2005.
9) Phoon, K. K. and Kulhawy, F. H.: Characterization of Geotechnical Variability, Canadian Geotechnical Journal, 36(4), 612-624, 1999.
10) Popescu, R., Prevost, J. H. and Deodatis, G.: Effects of Spatial Variability on Soil Liquefaction: Some Design Recommendations, Geotechnique, 47(5), 1019-1036, 1997.
11) Popescu, R., Prevost, J. H. and Deodatis, G.: 3D Effects in Seismic Liquefaction of Stochastically Variable Soil Deposits, Geotechnique, 55(1), 21-31, 2005.
12) Shinozuka, M. and Deodatis, G.: Simulation of Multi-dimensional Gaussian Fields by Spectral Representation, Applied Mechanics Reviews, ASME, 49(1), 29-53, 1996.
13) Vanmarcke, E.: Random Fields, MIT Press, Cambridge, MA, USA, 1984.

(Received September 1, 2017)